Heliyon 10 (2024) e36488

Contents lists available at ScienceDirect

Heliyon

journal homepage: www.cell.com/heliyon

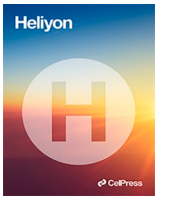

Research article

Knockout of TNF-α in microglia decreases ferroptosis and convert microglia phenotype after spinal cord injury

Fanzhuo Zeng [a,b,c], Anqi Chen [a,d], Wei Chen [a], Shuai Cheng [b], Sen Lin [b,***], Rongcheng Mei [a,d,**], Xifan Mei [b,*]

[a] *Department of Orthopedics, Xiangyang Central Hospital, Affiliated Hospital of Hubei University of Arts and Science, Xiangyang, 441021, Hubei, China*
[b] *Department of Orthopedics, The Third Affiliated Hospital of Jinzhou Medical University, Jinzhou, 121002, Liaoning, China*
[c] *Department of Neurobiology, School of Basic Medical Sciences, Guangdong-Hong Kong-Macao Greater Bay Area Center for Brain Science and Brain-Inspired Intelligence, Southern Medical University, Guangzhou, 510515, Guangdong, China*
[d] *Medical College of Wuhan University of Science and Technology, Wuhan, 430081, Hubei, China*

ARTICLE INFO

Keywords:
Spinal cord injury
TNF-α
Ferroptosis
Microglia
Apoptosis
Inflammation

ABSTRACT

Background: Spinal cord injury (SCI) is a serious and difficult to treat traumatic disease of the central nervous system. Spinal cord injury causes a variety of detrimental effects, including neuroinflammation and ferroptosis, leading to chronic functional impairment and death. Recent studies have shown that microglia/macrophages (M/Ms) at the injury site remain primarily in the pro-inflammatory state, which is detrimental to recovery. However, information on the factors behind pro-inflammatory polarization skew in the injured spinal cord remains unclear. In this study, we found that Tumor Necrosis Factor-α(TNF-α) ablation protected after SCI by suppressing neuroinflammation and ferroptosis. Though using TNF-α knock out mice (TNF−/−), we induced downregulation of TNF-α in M/Ms and further investigated its effect on SCI outcome. In TNF−/− mice, significant behavioral improvements were observed as early as 7 days after injury. We showed that TNF-α inhibition promote injury-mediated M/Ms polarization from pro-inflammatory to anti-inflammatory phenotype in vivo. Furthermore, accumulated iron in M/Ms after SCI increased the expression of TNF-α and the population of M/Ms to pro-inflammatory phenotype. Moreover, zinc supplement reduced the secondary damage caused by iron overload. In conclusion, we found that knock out of TNF-α promotes recovery of motor function after spinal cord injury in mice by inhibiting ferroptosis and promoting the shift of macrophages to an anti-inflammatory phenotype, indicating that there is great potential for this therapy to SCI.

1. Introduction

In the central nervous system (CNS), microglia serve as the dominant immune cells, responding promptly to injury within minutes [1–3]. In spite of the protective nature of their early response, these cells soon became pro-inflammatory and started a series of reactions that led to the entry of peripheral immune cells, predominantly the monocyte-macrophage lineage [4,5]. When microglia

* Corresponding author. Professor. Jinzhou Medical University, Jinzhou, Liaoning Province, China.
** Corresponding author. Xiangyang central hospital, Affiliated hospital of Hubei University of Arts and Science, Hubei Province, China.
*** Corresponding author. Jinzhou Medical University, Jinzhou, Liaoning Province, China.
E-mail addresses: aldrin_lin@163.com (S. Lin), meirch@163.com (R. Mei), meixifan@jzmu.edu.cn (X. Mei).

https://doi.org/10.1016/j.heliyon.2024.e36488
Received 12 May 2024; Received in revised form 8 August 2024; Accepted 16 August 2024
Available online 16 August 2024
2405-8440/© 2024 The Authors. Published by Elsevier Ltd. This is an open access article under the CC BY-NC-ND license (http://creativecommons.org/licenses/by-nc-nd/4.0/).

activation begins, their cytoplasmic processes contract, and the morphology and macrophages markers entering through the peripheral circulation to the damaged CNS are unable to be distinguished [6,7]. Injuries to the CNS can trigger macrophage responses resulting in auxiliary damage and functional impairment. However, macrophages may also play a protecting and regeneration-promoting role in the damaged central nervous system [8,9]. These double characters of macrophages are now deemed to be a result of their polarized state. The heterogeneous phenotype of macrophages ranges from "classically activated" pro-inflammatory, cytotoxic pro-inflammatory cells to "alternatively activated" anti-inflammatory, pro-reparative anti-inflammatory cells. Pro-inflammatory polarization is induced by Interferon-γ (IFN-γ), the prototypical T helper 1 (Th1) cytokine and the Toll-like receptor-4 (TLR-4), ligand lipopolysaccharide (LPS), while anti-inflammatory polarization is induced by the Th2 cytokine, Interleukin-4(IL-4), and other factors. It has been shown in previous studies that despite the presence of both pro-inflammatory and anti-inflammatory macrophages at the injury site, environment of the spinal cord facilitates the polarization of pro-inflammatory cytotoxic macrophages [10,11]. It has also been demonstrated that anti-inflammatory macrophages enter the injured site through a central pathway and exert neuroprotective properties after SCI [12–14]. It is essential to understand the reasons for the spinal cord environment's tendency to favor pro-inflammatory polarization in order to develop methods that could reduce pro-inflammatory polarization and promote protective anti-inflammatory polarization in order to promote rehabilitation following injury. The results of previous studies indicate that injury induces a shift from anti-inflammatory to pro-inflammatory cytokine expression [15,16]. How this damage affects macrophage and microglia polarization is unclear.

Ferroptosis is an iron-dependent programmed cell death caused by unrestricted phospholipid peroxidation, a process that occurs largely dependent on increased accumulation of the metabolite reactive oxygen species, phospholipids containing polyunsaturated fatty acid chains, and iron [17,18]. The concept of ferroptosis was first proposed by Prof. Brent Stockwell of Columbia University, and with increasing research on ferroptosis, it has been found that ferroptosis can lead to neuronal cell death, central nervous system damage, and neurological deficits in neurodegenerative diseases. During ferroptosis, glutathione (GSH) peroxidase 4 and glutathione levels decrease and reactive oxygen species 4-Hydroxynonenal (HNE) levels increase [19,20]. Previous studies have shown that microglia can exacerbate ferroptosis by promoting the expression of reactive oxygen species [21,22]. However, there is still a lack of valid evidence as to whether there is a relationship between inflammation and ferroptosis.

It was demonstrated in this paper that, even after time, M/Ms in the injured site still retain primarily pro-inflammatory polarization after SCI. We also showed that iron accumulation at high levels in M/Ms induced TNF-α expression and a switch from the anti-inflammatory phenotype to the pro-inflammatory phenotype. Studies have shown that zinc ions can reduce inflammation after spinal cord injury [23–25]. We observed the effect of zinc ion on ferroptosis after spinal cord injury in mice. We demonstrated that, by supplying zinc, pharmacological decrease of apoptosis and inflammation appears to mitigate secondary injury and maximize the extent of mitochondrial integrity for better function result. Therefore, our data supported that TNF-targeted therapy promotes neuroprotection in SCI.

2. Materials and methods

2.1. Animals and SCI model

Adult C57 BL/6J wild type (WT) mice, male and female, weighing 20–28 g, 8–10 weeks old, were purchased from Charles River (Zhejiang). The TNF-α KO mice were purchased from Jackson Lab, Strain number:005540. All the animal experiments in this work were performed in accordance with the Ethical Committee of Care and Use of Laboratory Animals at Jinzhou Medical University (Laboratory Animal Use License Number: SYXK 2019–0007). The control mice in this experiment were WT sham-operated mice (Sham-WT) and TNF-α knockout sham-operated mice (Sham-TNF−/−). A mouse spinal cord T10 segment contusion injury model was performed according to Allen's method, following a previously published procedure [23,24,26]. The mice were anesthetized using isoflurane under an anesthesia machine (induction concentration 3 %, maintenance concentration 1 %, flow rate 0.6–1L/min). Dorsal hair was removed, the area was disinfected with iodophor, and a 1.5 cm incision was made at the T10 segment of the spinal cord to locate the T10 vertebral body on the 10th rib. A T10 laminectomy was then performed to expose the spinal cord. Next, a homemade impactor (10 g) was used to strike the exposed spinal cord surface from a height of 1 cm in free fall. Mice in the sham-operated group were only stripped of their vertebral plates and not struck. Immediately after the contusion injury, edema and ecchymosis appeared, resulting in a reduction of the motor behavior score to 0 on the Basso mouse scale after awakening from anesthesia. The mice lost motor function in the hind limbs, developed urinary retention, and exhibited dragging of the hind limbs on the ground with an inability to lift the tail. The mice were sutured with cotton swabs to remove the exuded blood, and the fascia, muscle, and skin were sutured layer by layer. The mice were then disinfected again with iodophor. One hour after surgery, the control group mice were given intraperitoneal saline (0.1 mL), the iron treatment group mice were given intraperitoneal injections of Iron–Dextran (Aladdin, cat:I121237-250 g, 500 mg/kg body weight) for 7 days, the iron + zinc treatment group mice were given intraperitoneal injections with Iron–Dextran (500 mg/kg body weight) + ZnSO4 (Aladdin, cat: Z111853-500 g, 30 mg/kg body weight) for 7 days as previously published [25,27]. After surgery, each mouse was placed in a holding cage (on an insulating mat in winter until awakening) with feed placed on the matting for easy access. Following modeling, the bladders of the mice were manually emptied twice daily until they were euthanized.

2.2. Flow cytometry

Mice were anesthetized for execution using isoflurane. After a quick cold (4 °C) PBS perfusion, spinal cords of the mice were rapidly dissected out before, 3 days after or 7 days after the contusion. The central 5 mm of the lower thoracic lesion including the lesion core

and 2.5 mm rostral and caudal were then rapidly removed. The fluorescence activated cell sorting (FACS) staining was performed in accordance with standard procedures. Bovine serum albumin (5 % BSA) was used to block specific antibody binding. Tissues were dissociated using Neural Tissue Dissociation Kit and stained with CD45-FITC (BD Pharmingen, cat:553,080) and CD11b-APC-Cy7(BD Pharmingen, cat:557,657) for 10 min at 4 °C. Microglia were then FACS purified using the markers CD45 and CD11b. Analysis of cells was carried out using a FACS CantoII flow cytometer and FACS Diva software. The results were analyzed using FlowJo software.

2.3. Quantitative real-time PCR (RT-qPCR)

For quantitative real-time PCR (RT-qPCR) experiments, spinal cord tissue was obtained 7 days following injury. The total RNA was extracted using TRIzol reagent, and cDNA was synthesized from 5 μg total RNA. RT-qPCR was conducted using SYBR Green. Following are the conditions under which cDNA samples were amplified using a 7500 Rapid RT-PCR System (Applied Biosystems): 3 min at 95 °C followed by 40 cycles of 15 s at 95 °C and 45 s at 60 °C. In comparison of the target genes in experimental group, those in control group were applied with the method of $(1 + e)^{-\Delta\Delta CT}$, and the corresponding expression levels of those target genes were normalized to ribosomal protein S18 (RPS18), the relative expression of the housekeeping gene. In order to normalize the level of mRNA in the samples, the amount of RPS18 in the samples was used (comparison of RNA levels with corresponding controls). Primer information is shown in Table S1.

2.4. Histological analysis

The spinal cord tissues of mice were removed and fixed in 4 % buffered formaldehyde for histological analysis. Immunohistochemical staining was performed using paraffin-embedded spinal cord sections and analyzed with ImageJ. We determined the effect of knockdown of TNF-α on neuronal survival by Terminal deoxynucleotidyl transferase dUTP nick end labeling (TUNEL Test kits, Beyotime, cat:C1098) assay and Neuronal nuclei (Neun) immunofluorescence staining. a higher number of TUNEL positives indicates a higher number of apoptotic necrotic neurons, whereas a higher number of Neun positives indicates a higher number of surviving neurons. Dihydroethidium (DHE Test kits, Beyotime, cat: S0063) is the most commonly used fluorescent probe to detect intracellular superoxide anion levels, and we use it to detect reactive oxygen species (ROS) according to the manufacturer's instructions [28,29]. We calculated results using the number of surviving neurons per 0.05 mm^2. For immunofluorescence staining, sections were blocked with 5 % goat serum for 1 h at room temperature and then incubated with primary antibodies overnight at 4 °C. The following day, Alexa Fluor-488 and Alexa Fluor-568 were used to stain the tissues for 2 h at room temperature. Staining of the nuclei was performed using DAPI solution. 2 mm range of images were obtained above and below the site of the spinal cord injury. Cell counts were performed using unbiased stereology. A positive cell rate per 0.05 mm2 was used to calculate the results. Finally, the results were observed using a fluorescence microscope (Olympus VS200, Nikon C2 Confocal microscope). In order to calculate the absolute cell number counts and densities, the optical fractionator component of ImageJ software was utilized.

2.5. Enzyme linked immunosorbent assay (ELISA)

Mice were anesthetized for execution using isoflurane. After a quick cold (4 °C) PBS perfusion, spinal cords of the mice were rapidly dissected out before and after the contusion. The central 5 mm of the lower thoracic lesion including the lesion core and 2.5 mm rostral and caudal were then rapidly removed. Then extract the proteins. According to the manufacturer's instructions, protein extracts were prepared and TNF-α was measured using an ELISA kit (Proteintech, KE10002). These tissues were used to extract proteins and measure GSH (Elabscience, E-EL-0026) and HNE (Elabscience, E-EL-0128) in accordance with the manufacturer's instructions.

2.6. Behavioral test

2.6.1. Gait and motion analysis

The mice were video-recorded during walking through the left to right side on a runway bar (160 cm long, 10 cm wide, and 8 cm thick) at 1 day prior to and 1, 3, 4, 7, 14, 21 and 28 days post-SCI by CatWalk system for gait analysis [30,31]. The movement information of mice was collected separately, such as regularity index, max contact mean intensity, cadence and rump-height Index (RHI). The RHI is defined as the height of the rump. To minimize the variations of pre-surgery RHI of each animal, the standardized RHI (dividing post-injury value by pre-injury value) was applied for comparisons.

2.6.2. BMS score

Mice were assessed on the day before modeling of spinal cord injury, and on days 1, 3, 7, 14, 21, and 28 after modeling by two persons skilled in Basso Mouse Scale (BMS) scoring [32]. A score of 0 indicated no ankle and paw movement, and a score of 9 indicated normal motor function.

2.7. Statistical analysis

SPSS 23.0 was used for general data visualization and statistical analyses. Unpaired Student's *t*-test was used for simple comparisons, while one-way ANOVA or Two-way ANOVA with Bonferroni post-hoc test was utilized for multiple comparisons. BMS was analyzed using two-way repeated-measures ANOVA with Bonferroni post-hoc tests. Error bars in all figures represent mean ± SD (*$P <$

0.05, **$P < 0.01$, ***$P < 0.001$). A P-value <0.05 was considered statistically significant. Detailed information on the statistical methods for each experiment was described in the figure legends. All samples or animals were included in the statistical analysis. The number of mice in each group was n = 6.

3. Results

3.1. TNF-α ablation exacerbated functional recovery after SCI

After SCI (Fig. 1A), WT mice had a lower regularity index compared to TNF−/− mice (SCI-WT vs SCI-TNF−/−, $p < 0.001$) (Fig. 1B). At 28 dpi, between SCI-WT and SCI-TNF−/− mice, a significant improvement was noted (Fig. 1C), although we compared the cadence of the two groups and found that SCI-WT and SCI-TNF−/− mice revealed no difference (Fig. 1D). Next, we used behavioral tests to investigate whether TNF-α aggravates recovery after SCI. We found that SCI mice, especially TNF−/− mice, a significant improvement in rehabilitation of functional abilities was observed by the BMS score. This analysis showed that at 28 days after injury, the BMS score of SCI-WT mice was about 3 points, and the BMS score of SCI-TNF−/− mice increased to 6 points (Fig. 1E). The RHI analysis of SCI-TNF−/− mice was significantly improved from 7 dpi to 28 dpi compared with SCI-WT mice (Fig. 1F). Thus, SCI mice are prone to motor dysfunction and neuronal loss, and TNF-α deletion ameliorated these effects.

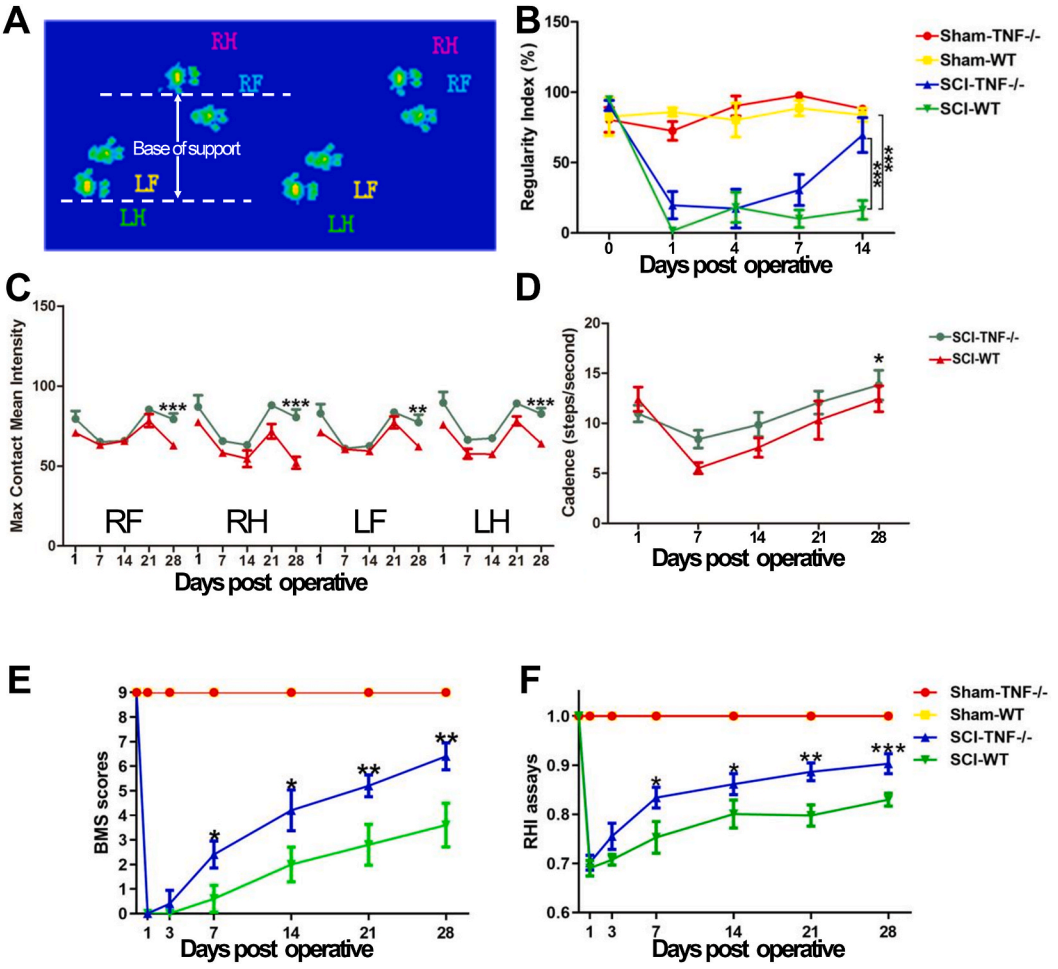

Fig. 1. Different function recovery are assessed after spinal cord injury in mice. (A) Footprints of mice containing four paws (RF: right forelimb, RH: right hindlimb, LF: left forelimb, LH: left hindlimb). The maximum contact area of each paw with the glass plate, the average width of support between hind paws, and the normal step ratio can be detected by illumination. (B) Representative quantification of the regularity index of Sham-WT, Sham-TNF−/−, SCI-WT, and SCI-TNF−/− mice. (C) Representative quantification of max contact mean intensity of SCI-WT and SCI-TNF−/− mice. (D) Representative quantification of cadence of SCI-WT and SCI-TNF−/− mice. (E) Representative quantification of BMS scores of Sham-WT, Sham-TNF−/−, SCI-WT, and SCI-TNF−/− mice. (F) Representative quantification of RHI assays of Sham-WT, Sham-TNF−/−, SCI-WT, and SCI-TNF−/− mice. (B–F) Two-way repeated-measures ANOVA with Bonferroni post-hoc tests. *, $P < 0.05$; **, $P < 0.01$; ***, $P < 0.001$. (n = 6). Error bars in all figures represent mean ± SD.

3.2. Microglia and macrophages at the injury site exhibited time-dependent distinct phenotypes after SCI

It has been shown in previous studies that pro-inflammatory M/Ms are predominantly polarized in the mice with SCI. Our study developed this project further to the cellular mRNA level by using FACS analysis (Fig. 2A) to measure expression of microglia and macrophage pro-inflammatory and anti-inflammatory markers on days 1, 3 and 7 after SCI. A series of time points were selected to study early microglial responses before macrophage influx (1 day), early peripheral macrophage infiltration (3 days), and early microglial responses after macrophage influx. Results showed that macrophages (CD11b+, CD45high) and microglia (CD11b+, CD45low) expressed pro-inflammatory markers such as inducible nitric oxide synthase (iNOS), TNF-α, and CD86 in a much higher proportion than anti-inflammatory markers such as Arginase-1(Arg-1), CD206, and Transforming growth factor β(TGF-β). From 1 to 7 days after SCI, macrophages from the peripheral circulation increased significantly in the expression of pro-inflammatory markers (iNOS), and the maximum value reached was approximately 4 % (Fig. 2B). A dramatic increase of CD86, an additional pro-inflammatory marker, was observed in macrophages 3 days post injury, with a peak increase of about 20 % by the 7th day (Fig. 2C). A consistent growth of the pro-inflammatory marker TNF-α was observed in macrophages after SCI, while by the seventh day, the increase had reached a maximum of approximately 10 % (Fig. 1D). In contrast, pro-inflammatory markers in microglia, iNOS

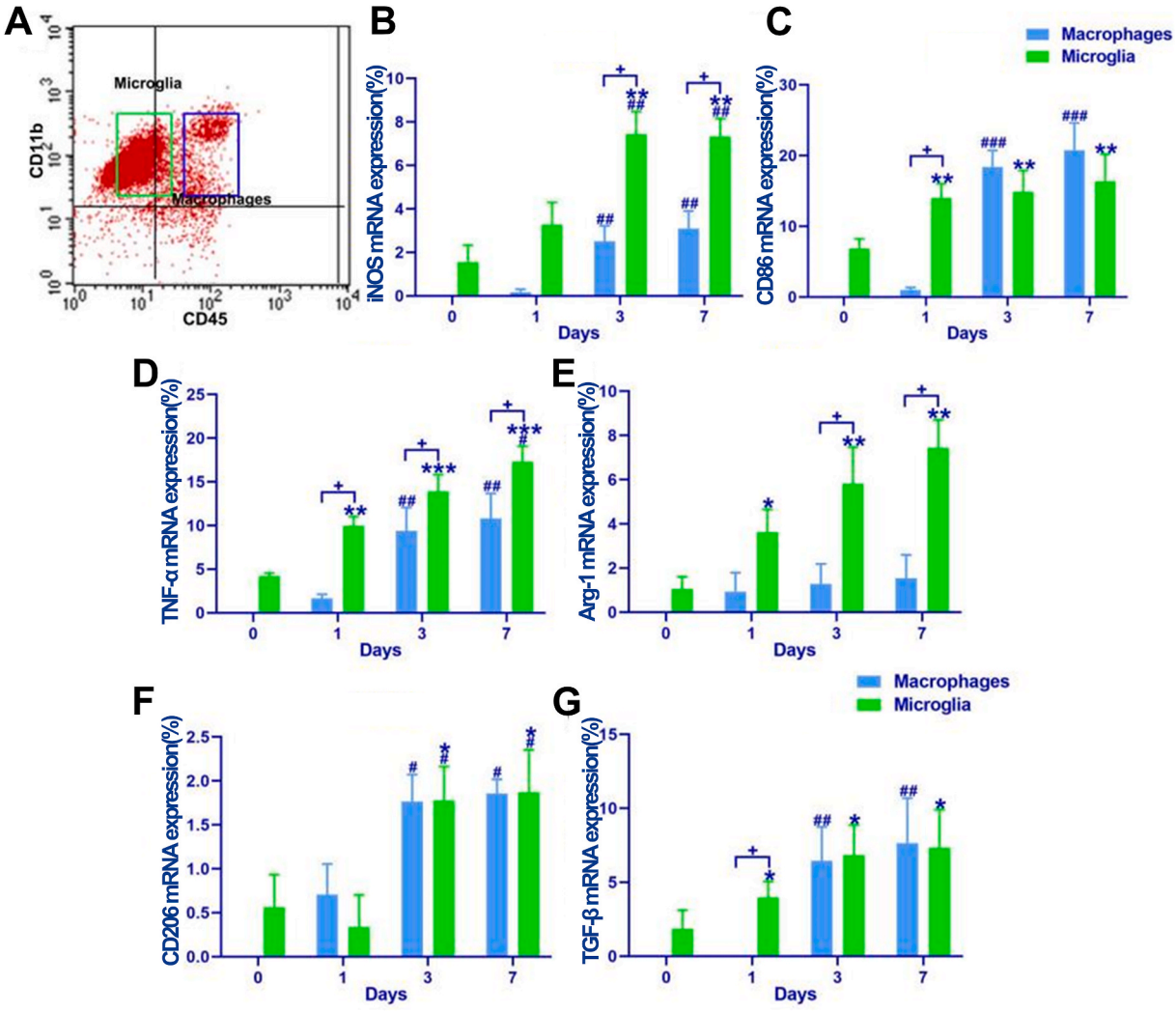

Fig. 2. Pro-inflammatory markers predominantly expressed after SCI. (A) Representative images of CD11b+, CD45^{+} macrophages/microglia. Blue Gate displayed CD45high (macrophages) and green gate display CD45low cells (microglia). (B)Quantification of expressions of iNOS mRNA in macrophages and microglia. (C)Quantification of expressions of CD86 mRNA in macrophages and microglia. (D)Quantification of expressions of TNF-α mRNA in macrophages and microglia. (E)Quantification of expressions of Arg-1 mRNA in macrophages and microglia. (F)Quantification of expressions of CD206 mRNA in macrophages and microglia. (G)Quantification of expressions of TGF-β mRNA in macrophages and microglia. (B–G) Two-way repeated-measures ANOVA with Bonferroni post-hoc tests. *, significant difference compared to day 0 (*, $P < 0.05$; **, $P < 0.01$; ***, $P < 0.001$); #, compared to day 1 (#, $P < 0.05$; ##, $P < 0.01$; ###, $P < 0.001$); +, significant difference between macrophages and microglia (+, $P < 0.05$). (n = 6). Error bars in all figures represent mean ± SD.

expression level was about 7 %, TNF-α expression level was about 18 %, and CD86 expression level was about 17 %, respectively (Fig. 2B–D). Based on these findings, it is concluded that microglia display a higher degree of stability in the expression of pro-inflammatory markers than macrophages in the acute phase of SCI. A further finding was that the anti-inflammatory markers were expressed exclusively within the microglia and macrophages of the injured site. Arg-1 expression was approximately 4 % in microglia on day 1, progressively increasing to 8 % on day 7 (Fig. 2E), and below 2 % in macrophages. In macrophages and microglia, CD206 was expressed at a level of approximately 2 % (Fig. 2F). TGF-β was consistently expressed by about 8 % in macrophages and microglia at day 7 (Fig. 2G). The research showed that pro-inflammatory polarization was detrimental to damaged lesions after SCI.

3.3. Continuous TNF-α ablation promotes the survival of neurons and myelin sheath

We have shown that pro-inflammatory polarization in injured SCI is a distinguishing feature of the acute SCI phase. Therefore, we intended to investigate if sustained ablation of TNF-α could prevent the cytopathic response to traumatic SCI. Compared with sham mice (132.37 ± 20.14 NeuN + cells), we measured a significant decrease in NeuN-positive cells (58.02 ± 12.36 NeuN + cells) in WT mice after SCI, while there was no difference between sham-TNF−/−mice (151.36 ± 26.20 NeuN+) and SCI-TNF−/−mice (116.15 ± 21.36 NeuN + cells) (Fig. 3A and B). Our measurements of GFAP levels in WT and TNF−/− mice were conducted since this protein is known to be one of the major proteins required by astrocytes [33]. The results of our study indicated that SCI significantly increased the expression of GFAP in SCI-WT mice (approximately 1.97fold of sham-WT mice), and this effect was improved in SCI-TNF−/− mice (approximately 1.78fold of sham-TNF−/− mice), which also showed that the amount of GFAP was decreased, but significantly higher than that in WT mice (Fig. 3A and C). Further investigation of the association between demyelination inhibition and increased oligodendrocyte survival in TNF−/− mice was carried out by performing immunohistochemical assays with anti-myelin basic protein (MBP) antibody. Quantification of MBP immunoreactivity indicated that SCI led to a significant loss of MBP-positive cells in the injured spinal cord (Fig. 3A and D). In comparison with SCI-WT mice, the number of MBP-positive cells (563.17 ± 142.39 MBP cells) was significantly higher in SCI-TNF−/− mice (Fig. 3A and D). These results showed that sustained TNF-α ablation protected nerve cells in the injured spinal cord.

3.4. TNF-α ablation decreases neuroinflammation and ferroptosis

Numerous researches have demonstrated that TNF-α can play a role in many pathological processes by regulating ferroptosis [33–35]. However, the role of TNF-α on ferroptosis in M/Ms after SCI is unclear. A significant increase was observed for CD11b + cells

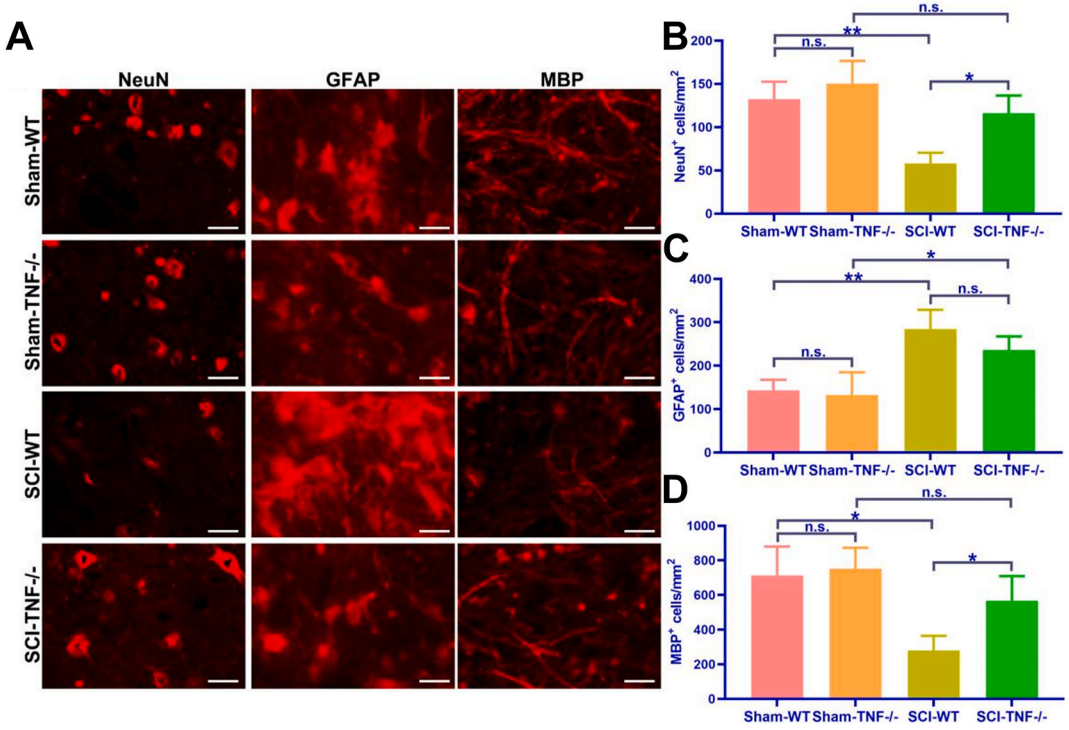

Fig. 3. Sustained TNF-α ablation protects injured spinal cord. (A) Representative images of NeuN+, GFAP+ and MBP + cells on 7th day post-SCI. Scale bar = 200 μm. (B)Quantification of expression of NeuN on 7th day post-SCI. (C) Quantification of expression of GFAP on 7th day post-SCI. (D) Quantification of expression of MBP on 7th day post-SCI. (B–D) One-way ANOVA with Bonferroni post-hoc tests. *, $P < 0.05$; **, $P < 0.01$; ***, $P < 0.001$; ns = no significance. (n = 6). Error bars in all figures represent mean ± SD.

in WT mice after SCI (278.39 ± 34.06 CD11b + cell), compared with sham mice (92.36 ± 14.55 CD11b + cell), and a significant decrease for CD11b + cells in TNF−/− mice after SCI (168.07 ± 23.07 CD11b + cell) as compared with SCI-WT mice (Fig. 4A and B). Due to the fact that Arg-1 protein is recognized as being one of the major proteins involved in the anti-inflammatory phenotype, we determined the percentage of CD11b + cells positive for Arg-1. Our results showed that SCI increased the expression of Arg-1 in WT mice, and this effect was considerably improved in TNF−/− mice (Fig. 4A and C). To further investigate whether ablation of TNF is associated with downregulation of ferroptosis in SCI mice, we tested the expressions of GSH and HNE by performing ELISA analysis. We found significant changes in GSH and HNE expression in SCI-TNF−/− mice in comparison to SCI-WT mice (Fig. 4D and E). The results showed that continuous TNF-α ablation had anti-inflammatory and anti-ferroptosis effects on injured spinal cord.

3.5. Increased intracellular iron influences TNF-α expression and macrophage polarization

Hemorrhages and extravasation of red blood cells (RBCs) occur as a result of spinal cord contusions [36], which are quickly engulfed by macrophages. It is also possible for dead cells to release iron, which is then absorbed by macrophages. Iron-binding and storage protein ferritin, whose expression increases in the presence of elevated intracellular iron, is an excellent surrogate marker for intracellular iron. We examined TNF-α expression in ferritin+, CD11b + M/Ms at 7 days after SCI. What's interesting is the number of TNF+/ferritin + M/Ms was 2–3 fold higher than that of ferritin-/CD11b + cells (Fig. 5A and B), and the majority of ferritin + CD11b + cells expressed TNF-α. In the knockout of TNF-α (TNF−/− mice), Arg-1 was increased by 20 % in iron-containing CD11b + M/Ms and pro-inflammatory marker CD86 was significantly reduced (12 %) as compared to WT mice (Fig. 5C–F). It was concluded from these studies that TNF-α increased pro-inflammatory and decreased anti-inflammatory polarization, especially in iron-containing M/Ms in the injured spinal cord. Following SCI, many M/Ms are already iron-loaded due to phagocytosis of red blood cells that bleed into the tissue. Using systemic treatment with iron-dextran, we investigated whether further increasing iron load would result in altered TNF-α expression and poorer prognosis after SCI. For 7 days after injury, mice were injected intraperitoneally with 500 mg/kg body weight of iron-dextran daily. An increase in iron deposition was observed in the injured spinal cord of iron dextran-treated mice compared with dextran-treated control mice based on the results of the iron histochemistry (Fig. 5G). Strikingly, 4-fold increased TNF-α expression in the mice treated with iron-dextran was detected by ELISA in comparison with control (dextran-treated) mice (Fig. 5H). Despite already high iron levels in red blood cells due to hemorrhage, systemic iron treatment in SCI mice worsened exercise recovery in comparison with vehicle-treated SCI controls. As a result of BMS analysis, iron-treated mice for 7 days and 28 days had poorer motor recovery than controls (Fig. 5I).

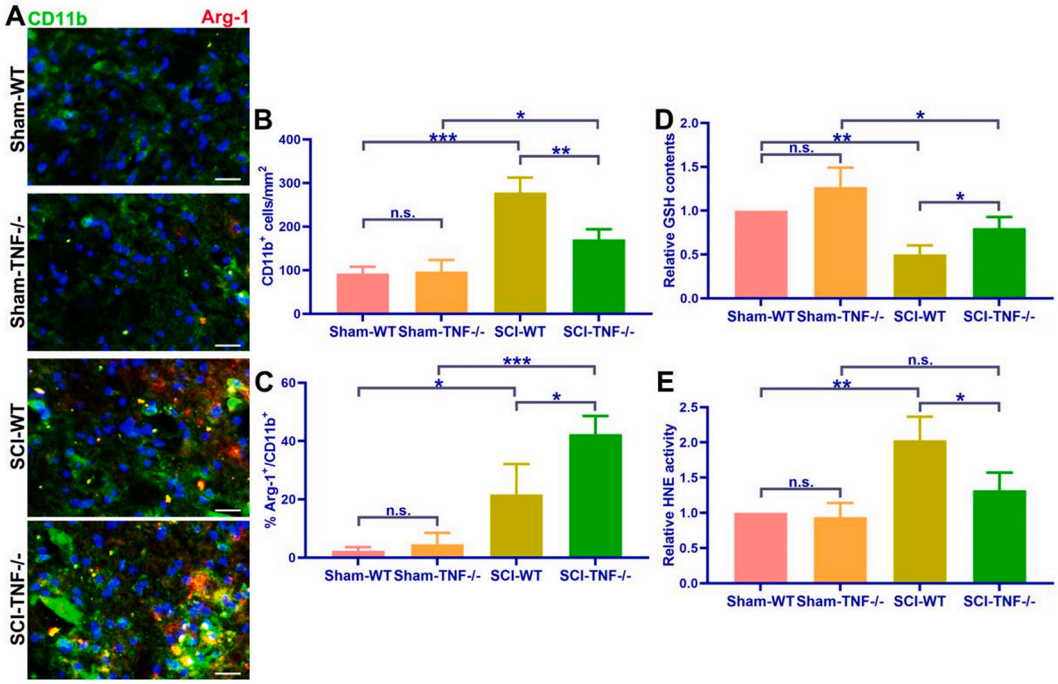

Fig. 4. Anti-inflammation and anti-ferroptosis effects of TNF-α ablation in SCI mice. (A) Representative images of CD11b+ and Arg-1+ cells on 7th day post-SCI. Scale bar = 200 μm. (B)Quantification of the expression of CD11b on 7th day post-SCI. (C) Quantification of the expression of Arg-1/CD11b on 7th day post-SCI. (D–E) Quantification on the expression of GSH and HNE at 7th day post-SCI. (B–E) One-way ANOVA with Bonferroni post-hoc tests. *, $P < 0.05$; **, $P < 0.01$; ***, $P < 0.001$. (n = 6). Error bars in all figures represent mean ± SD.

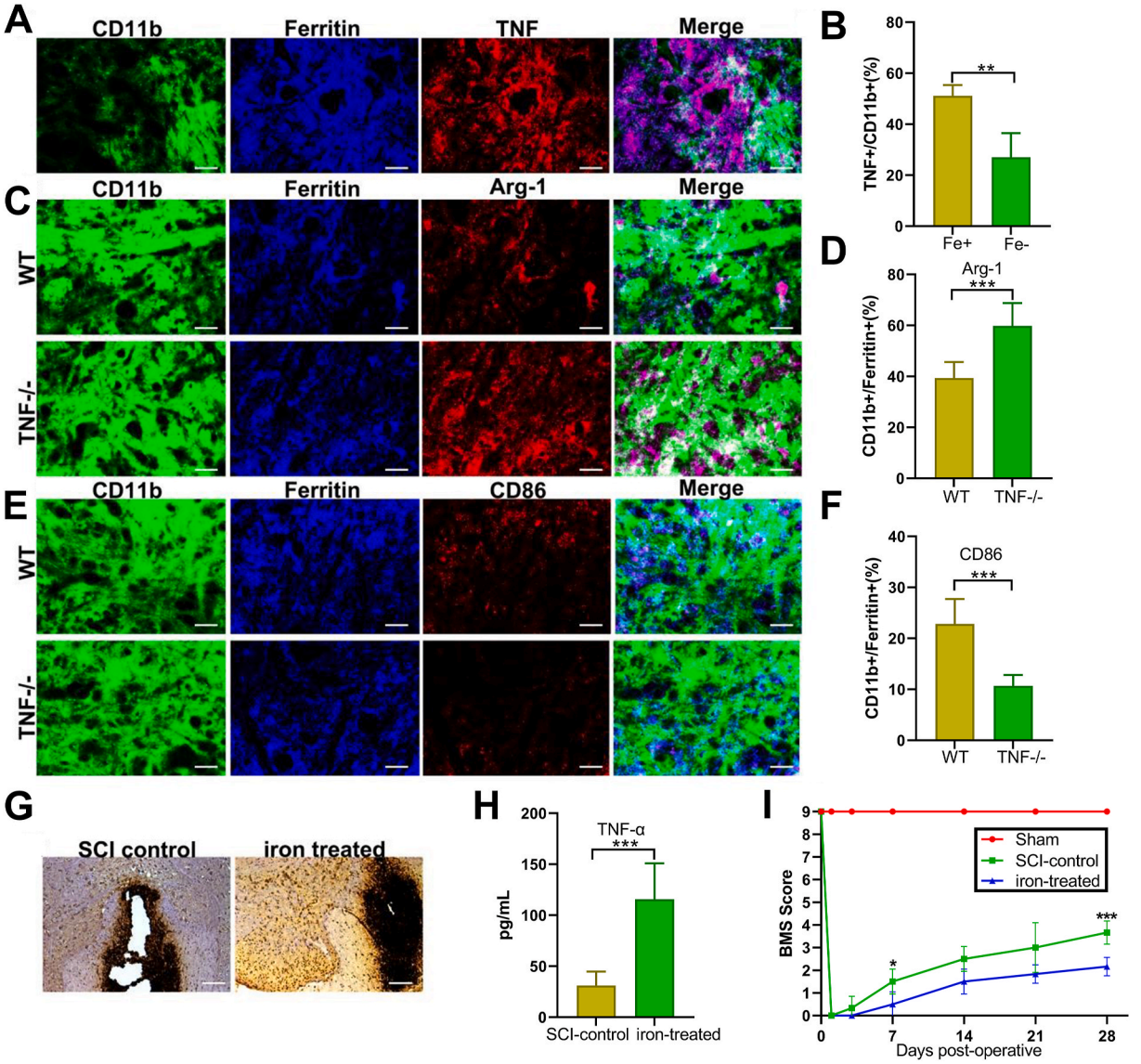

Fig. 5. Increased Intracellular Iron Influences TNF-α Expression and Macrophage Polarization. (A)Representative images of CD11b+, ferritin+ and TNF + cells on 7th day post-SCI. Scale bar = 200 μm. (B)Quantification of the expression of CD11b/TNF-α in ferritin + or ferritin-cells on 7th day post-SCI. (C)Representative images of Arg-1+, CD11b+,ferritin + cells on 7th day post-SCI. Scale bar = 200 μm. (D)Quantification of the expression of Arg-1 in CD11b+/ferritin + cells on 7th day post-SCI. (E)Representative images of $CD86^{+}$,CD11b+,/ferritin + cells on 7th day post-SCI. Scale bar = 200 μm. (F)Quantification of the expression of CD86 in CD11b+/ferritin + cells on 7th day post-SCI. (G)Representative images of iron histochemistry on 7th day post-SCI. Scale bar = 200 μm. (H)Quantification of the level of TNF-α on 7th day post-SCI.(I)quantification of BMS in SCI control and iron treated mice. (B, D, F, H) Student's unpaired *t*-test. (I)Two-way repeated-measures ANOVA with Bonferroni post-hoc tests. *, $P < 0.05$; **, $P < 0.01$; ***, $P < 0.001$. (n = 6). Error bars in all figures represent mean ± SD.

3.6. Effects of zinc treatment on the increasing of intracellular iron and TNF-α expression and in vivo functional outcomes after SCI

7 days following SCI, functional consequences of iron treatment were observed at the cellular level in the spinal cord, as iron-treated mice revealed a higher level of production of ROS detected utilizing DHE oxidation as a marker (Fig. 6A and B). Besides, iron-treated mice revealed a higher level of TUNEL staining (Fig. 6C and D), increased TNF-α expression detected by Immunohistochemistry (IHC) staining (Fig. 6E and F), and more damaged mitochondria (Fig. 6G) in comparison to vehicle-treated SCI controls, whereas zinc treatment improved these effects. Furthermore, zinc treatment also downregulated the expression of IL-6 and TNF-α mRNA compared with iron-treated mice (Fig. 6H). These data suggest that zinc restores SCI-induced iron load in acute SCI.

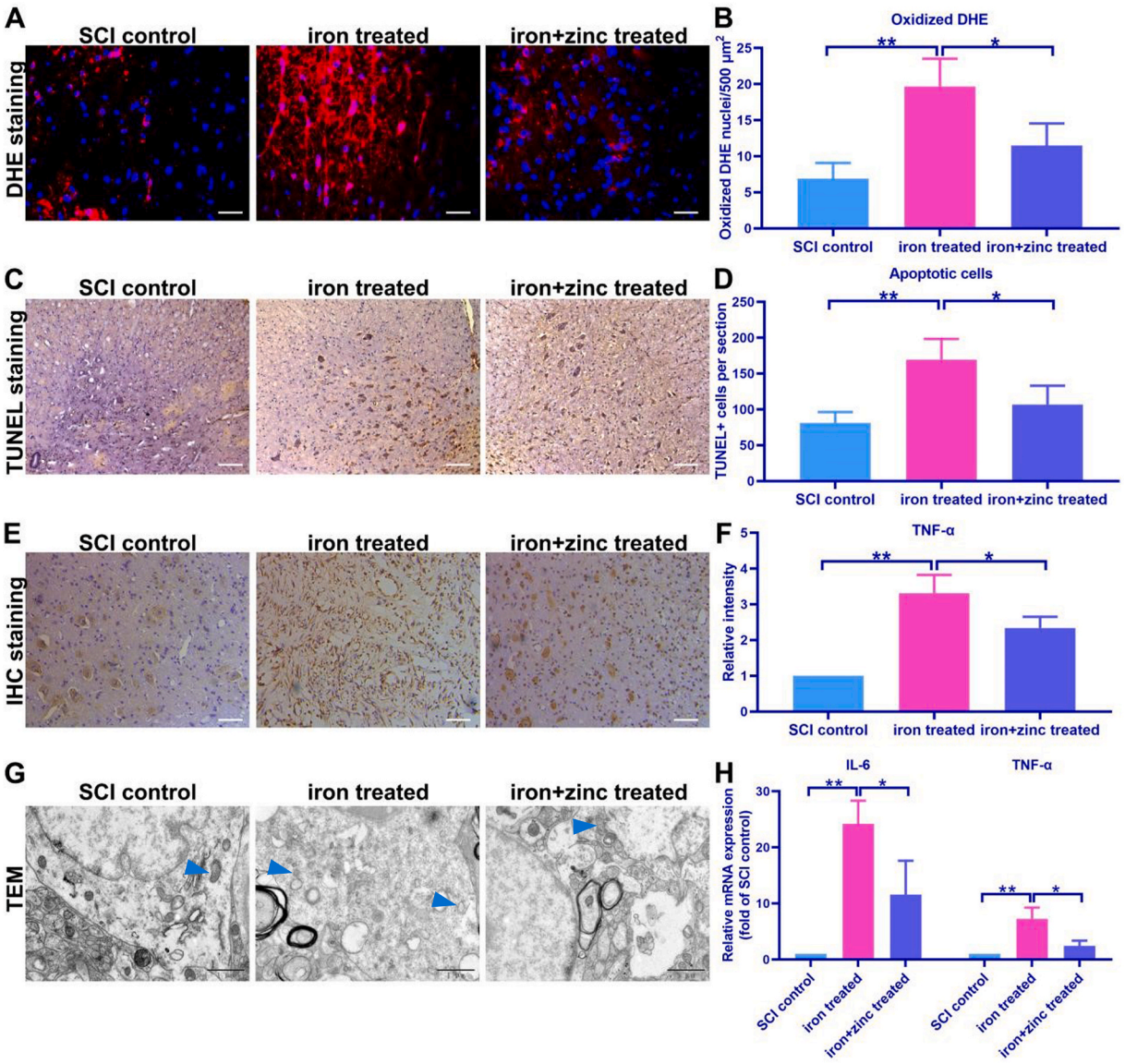

Fig. 6. Zinc treatment influence increased intracellular Iron and TNF-α expression and functional outcome in vivo after SCI. (A–B) The representative images and quantification of ROS were detected by DHE staining on the 7th day after spinal cord injury. Blue, DAPI. Red, ROS marked by DHE. Scale bar = 200 μm. (C–D) Representative images and quantification of TUNEL staining on 7th day post-SCI. Scale bar = 200 μm. (E–F) Representative image and quantification of TNF-α expression via IHC staining on 7th day post-SCI. Scale bar = 200 μm. (G)Representative images of damaged mitochondria on 7th day post-SCI. Blue arrow, mitochondria. Scale bar = 500 nm. (H)Quantification of expression of IL-6 and TNF-α mRNA on 7th day post-SCI. (B, D, F, H) One-way ANOVA with Bonferroni post-hoc tests. Error bars in all figures represent mean ± SD. (n = 6); *, $P < 0.05$; **, $P < 0.01$; ***, $P < 0.001$.

4. Discussion

M/Ms are viewed as the main primary immune cells in CNS diseases, especially SCI [36]. There are numerous pro-inflammatory cytokines and free radicals released by M/Ms that resulting in secondary damage and aggravate the progression of SCI [37,38]. However, under some specific experimental conditions M/Ms exhibit anti-inflammatory polarization, as a result of activation, and function to promote regeneration. Therefore, it is imperative that the polarization of M/Ms after injury is regulated and maintained in a manner that promotes neuroprotection and tissue repair. According to recent reports, the polarization of M/Ms in the injured spinal cord results in a variety of M/Ms [39–41], which is largely a consequence of cytokine production in the injury microenvironment. The results of the present study indicate that M/Ms predominantly exhibited a pro-inflammatory cytotoxic phenotype. In spite of macrophages infiltrating the injured site, most of them were derived from peripheral blood and clearly assumed a pro-inflammatory state as soon as the injury occurs. The primary pro-inflammatory response has been reported to substantially resulting in injuries to the

tissues and functional impairment [42–44]. Moreover, results of the research demonstrated that on day 7 after SCI, microglia switched to anti-inflammatory polarization. It is noteworthy that the data indicated that on day 7 post-injury, there was a considerable reduction in the expression of pro-inflammatory cytokines marked as pro-inflammatory status. However, the neurotoxic role of pro-inflammatory M/Ms during SCI development is unclear, and in vivo experiments, abolition of M/Ms improved functional recovery. These studies demonstrate that specific cytokines are able to respond to rapid changes in the microenvironment following acute trauma. As indicated by these sorted cell results, a mRNA level expression was observed at M/Ms and continued to increase M/Ms in the acute phase of SCI. There is evidence that TNF-α, a protein that functions as paracrine and autocrine agents, triggers inflammatory responses in M/Ms. It is interesting to note that, in vivo, TNF-α ablation promoted both upregulation of the anti-inflammatory marker Arg-1 and downregulation of the M/Ms-specific marker CD11b and the pro-inflammatory marker iNOS. Furthermore, there was a greater functional recovery for TNF−/− mice after injury compared to WT mice. Some of our experimental results are similar to those of previous studies, for example, it has been previously shown that TNF-α promotes the shift of microglia to an M1 pro-inflammatory phenotype and that intracellular iron also promotes the shift of microglia to an M1 pro-inflammatory phenotype [45]. As well, TNF-α expression is upregulated in CNS disorders such as multiple sclerosis, spinal cord injury and traumatic brain injury, correlates with poor prognosis and pathologic impairment. It has also been previously shown that ferroptosis, an iron-dependent form of cell death characterized by iron accumulation, lipid peroxidation, and irreversible plasma membrane disruption, contributes to the exacerbation of CNS disorders by accelerating neuronal dysfunction and aberrant microglia activation [46]. In this context, disturbances in brain iron homeostasis and neuronal ferroptosis exacerbate neuroinflammation and lead to abnormal microglia activation. Abnormally activated microglia release various pro-inflammatory factors that exacerbate iron homeostasis dysregulation and neuroinflammation, forming a vicious cycle. Our data in the present experiments demonstrated that microglia modulate the pathological manifestations of spinal cord injury through the inflammation-oxidative stress-ferroptosis axis. The limitation of this experiment is that we have taken a predominantly spinal cord percussion injury model, and knockdown of TNF-α reduces iron death and decreases neuronal loss caused by inflammatory storms secondary to injury, but the efficacy is likely to be relatively small for complete transecting spinal cord injuries.

It has also been found in this study that iron supplementation promoted TNF-α expression in the spinal cord after injury. To determine the level of intracellular iron, iron staining was used as a surrogate marker. Elevated intracellular iron levels also increased apoptosis and mitochondrial destruction in injured spinal cord. Interestingly, after zinc treatment, our study revealed that increased intracellular zinc favored the downregulation of the in vivo expression of TNF-α after SCI and reduced inflammatory expression.

It is thus concluded that TNF-α plays an important role in long-term maintenance of the anti-inflammatory neuroprotective properties possessed by anti-inflammatory M/Ms in the injured spinal cord, and offers a new strategy for treating spinal cord injury.

5. Conclusions

For the purpose of investigating whether TNF-α plays a role in the potentially pathogenic development of SCI, we used FACS analysis and showed that pro-inflammatory-related cytokines, especially TNF-α, were consistently increased in progressive SCI. After ablation of SCI mice with TNF-α, a decrease in pro-inflammatory-related proteins and M/Ms and a significant increase in mitochondrial metabolism were observed. The ROS analysis and mitochondrial staining indicated that TNF-α represents a neuroinflammatory signature in the injured spinal cords of WT mice that have been given iron supplementation treatment or not. Furthermore, these data confirm the tight relationship between TNF-α, iron and zinc in SCI. In summary, our research suggests that knock out of TNF-α promotes recovery of motor function after spinal cord injury in mice by inhibiting ferroptosis and promoting the shift of macrophages to an anti-inflammatory phenotype, suggests that TNF-α inhibition is a potential strategy for SCI therapy.

Funding

This work was supported by National Natural Science Foundation of China (NO. 82072165 and 82272256). This work was supported by the key project of Xiangyang Central Hospital, project approval number: 2023YZ03.

Ethics statements

All of the mouse experiments were conducted in accordance with the guidelines of the Institutional Animal Care and Use Committee of Jinzhou Medical University (Ethical Approval number:2022017).

Data availability statement

Most of the data sets that support the conclusions of this article are included in this article. The data sets analyzed during the current study are available from the corresponding author. Data will be made available on request.

CRediT authorship contribution statement

Fanzhuo Zeng: Writing – original draft, Methodology, Formal analysis, Conceptualization. **Anqi Chen:** Methodology, Investigation, Formal analysis. **Wei Chen:** Investigation, Formal analysis, Conceptualization. **Shuai Cheng:** Investigation, Formal analysis, Data curation. **Sen Lin:** Writing – review & editing, Resources, Investigation, Formal analysis, Conceptualization. **Rongcheng Mei:** Writing

– review & editing, Supervision, Resources, Data curation. **Xifan Mei:** Writing – review & editing, Supervision, Resources, Project administration, Data curation.

Declaration of competing interest

The authors declare that they have no known competing financial interests or personal relationships that could have appeared to influence the work reported in this paper.

Acknowledgements

Thanks to Jinzhou Medical University public experimental platform and Xiangyang Central Hospital Central laboratory teachers for their help and experimental conditions.

Appendix A. Supplementary data

Supplementary data to this article can be found online at https://doi.org/10.1016/j.heliyon.2024.e36488.

References

[1] C. Madore, Z. Yin, J. Leibowitz, O. Butovsky, Microglia, lifestyle stress, and neurodegeneration, Immunity 52 (2) (2020) 222–240.
[2] Q.M. Pang, S.Y. Chen, Q.J. Xu, M. Zhang, D.F. Liang, S.P. Fu, J. Yu, Z.L. Liu, Q. Zhang, T. Zhang, Effects of astrocytes and microglia on neuroinflammation after spinal cord injury and related immunomodulatory strategies, Int. Immunopharm. 108 (2022) 108754.
[3] J. Scholz, A. Abele, C. Marian, A. Haussler, T.A. Herbert, C.J. Woolf, I. Tegeder, Low-dose methotrexate reduces peripheral nerve injury-evoked spinal microglial activation and neuropathic pain behavior in rats, Pain 138 (1) (2008) 130–142.
[4] P.J. Murray, Macrophage polarization, Annu. Rev. Physiol. 79 (2017) 541–566.
[5] J.C. Gensel, B. Zhang, Macrophage activation and its role in repair and pathology after spinal cord injury, Brain Res. 1619 (2015) 1–11.
[6] X. Hu, R.K. Leak, Y. Shi, J. Suenaga, Y. Gao, P. Zheng, J. Chen, Microglial and macrophage polarization-new prospects for brain repair, Nat. Rev. Neurol. 11 (1) (2015) 56–64.
[7] J. Lyu, D. Xie, T.N. Bhatia, R.K. Leak, X. Hu, X. Jiang, Microglial/Macrophage polarization and function in brain injury and repair after stroke, CNS Neurosci. Ther. 27 (5) (2021) 515–527.
[8] Y. Li, X. He, R. Kawaguchi, Y. Zhang, Q. Wang, A. Monavarfeshani, Z. Yang, B. Chen, Z. Shi, H. Meng, S. Zhou, J. Zhu, A. Jacobi, V. Swarup, P.G. Popovich, D. H. Geschwind, Z. He, Microglia-organized scar-free spinal cord repair in neonatal mice, Nature 587 (7835) (2020) 613–618.
[9] X. Zhou, S. Wahane, M.S. Friedl, M. Kluge, C.C. Friedel, K. Avrampou, V. Zachariou, L. Guo, B. Zhang, X. He, R.H. Friedel, H. Zou, Microglia and macrophages promote corralling, wound compaction and recovery after spinal cord injury via Plexin-B2, Nat. Neurosci. 23 (3) (2020) 337–350.
[10] S. David, A. Kroner, Repertoire of microglial and macrophage responses after spinal cord injury, Nat. Rev. Neurosci. 12 (7) (2011) 388–399.
[11] X. Kong, J. Gao, Macrophage polarization: a key event in the secondary phase of acute spinal cord injury, J. Cell Mol. Med. 21 (5) (2017) 941–954.
[12] M.J. Kwon, H.J. Yoon, B.G. Kim, Regeneration-associated macrophages: a novel approach to boost intrinsic regenerative capacity for axon regeneration, Neural Regen Res 11 (9) (2016) 1368–1371.
[13] W. Miao, Y. Zhao, Y. Huang, D. Chen, C. Luo, W. Su, Y. Gao, IL-13 ameliorates neuroinflammation and promotes functional recovery after traumatic brain injury, J. Immunol. 204 (6) (2020) 1486–1498.
[14] R. Heinz, S. Brandenburg, M. Nieminen-Kelha, I. Kremenetskaia, P. Boehm-Sturm, P. Vajkoczy, U.C. Schneider, Microglia as target for anti-inflammatory approaches to prevent secondary brain injury after subarachnoid hemorrhage (SAH), J. Neuroinflammation 18 (1) (2021) 36.
[15] M. Ghosh, Y. Xu, D.D. Pearse, Cyclic AMP is a key regulator of M1 to M2a phenotypic conversion of microglia in the presence of Th2 cytokines, J. Neuroinflammation 13 (2016) 9.
[16] S. Xu, W. Zhu, M. Shao, F. Zhang, J. Guo, H. Xu, J. Jiang, X. Ma, X. Xia, X. Zhi, P. Zhou, F. Lu, Ecto-5'-nucleotidase (CD73) attenuates inflammation after spinal cord injury by promoting macrophages/microglia M2 polarization in mice, J. Neuroinflammation 15 (1) (2018) 155.
[17] S.J. Dixon, K.M. Lemberg, M.R. Lamprecht, R. Skouta, E.M. Zaitsev, C.E. Gleason, D.N. Patel, A.J. Bauer, A.M. Cantley, W.S. Yang, B. Morrison 3rd, B. R. Stockwell, Ferroptosis: an iron-dependent form of nonapoptotic cell death, Cell 149 (5) (2012) 1060–1072.
[18] H.N. Bell, B.R. Stockwell, W. Zou, Ironing out the role of ferroptosis in immunity, Immunity 57 (5) (2024) 941–956.
[19] X. Jiang, B.R. Stockwell, M. Conrad, Ferroptosis: mechanisms, biology and role in disease, Nat. Rev. Mol. Cell Biol. 22 (4) (2021) 266–282.
[20] J. Li, F. Cao, H.L. Yin, Z.J. Huang, Z.T. Lin, N. Mao, B. Sun, G. Wang, Ferroptosis: past, present and future, Cell Death Dis. 11 (2) (2020) 88.
[21] Z.L. Wang, L. Yuan, W. Li, J.Y. Li, Ferroptosis in Parkinson's disease: glia-neuron crosstalk, Trends Mol. Med. 28 (4) (2022) 258–269.
[22] S.K. Ryan, M. Zelic, Y. Han, E. Teeple, L. Chen, M. Sadeghi, S. Shankara, L. Guo, C. Li, F. Pontarelli, E.H. Jensen, A.L. Comer, D. Kumar, M. Zhang, J. Gans, B. Zhang, J.D. Proto, J. Saleh, J.C. Dodge, V. Savova, D. Rajpal, D. Ofengeim, T.R. Hammond, Microglia ferroptosis is regulated by SEC24B and contributes to neurodegeneration, Nat. Neurosci. 26 (1) (2023) 12–26.
[23] M.H. Ge, H. Tian, L. Mao, D.Y. Li, J.Q. Lin, H.S. Hu, S.C. Huang, C.J. Zhang, X.F. Mei, Zinc attenuates ferroptosis and promotes functional recovery in contusion spinal cord injury by activating Nrf2/GPX4 defense pathway, CNS Neurosci. Ther. 27 (9) (2021) 1023–1040.
[24] C. Xu, Z. Zhou, H. Zhao, S. Lin, P. Zhang, H. Tian, X. Mei, Zinc promotes spinal cord injury recovery by blocking the activation of NLRP3 inflammasome through SIRT3-mediated autophagy, Neurochem. Res. 48 (2) (2023) 435–446.
[25] S. Lin, H. Tian, J. Lin, C. Xu, Y. Yuan, S. Gao, C. Song, P. Lv, X. Mei, Zinc promotes autophagy and inhibits apoptosis through AMPK/mTOR signaling pathway after spinal cord injury, Neurosci. Lett. 736 (2020) 135263.
[26] A.R. Allen, Surgery of experimental lesion of spinal cord equivalent to crush injury of fracture dislocation of spinal column: a preliminary report, JAMA (1911) 878–880.
[27] G. Xing, L. Meng, S. Cao, S. Liu, J. Wu, Q. Li, W. Huang, L. Zhang, PPARalpha alleviates iron overload-induced ferroptosis in mouse liver, EMBO Rep. 23 (8) (2022) e52280.
[28] H. Liu, Y. Li, S. Sun, Q. Xin, S. Liu, X. Mu, X. Yuan, K. Chen, H. Wang, K. Varga, W. Mi, J. Yang, X.D. Zhang, Catalytically potent and selective clusterzymes for modulation of neuroinflammation through single-atom substitutions, Nat. Commun. 12 (1) (2021) 114.
[29] W. Chen, X. Shen, Y. Hu, K. Xu, Q. Ran, Y. Yu, L. Dai, Z. Yuan, L. Huang, T. Shen, K. Cai, Surface functionalization of titanium implants with chitosan-catechol conjugate for suppression of ROS-induced cells damage and improvement of osteogenesis, Biomaterials 114 (2017) 82–96.
[30] E. Kunkel-Bagden, H.N. Dai, B.S. Bregman, Methods to assess the development and recovery of locomotor function after spinal cord injury in rats, Exp. Neurol. 119 (2) (1993) 153–164.

[31] E.J. Bradbury, L.D. Moon, R.J. Popat, V.R. King, G.S. Bennett, P.N. Patel, J.W. Fawcett, S.B. McMahon, Chondroitinase ABC promotes functional recovery after spinal cord injury, Nature 416 (6881) (2002) 636–640.
[32] D.M. Basso, L.C. Fisher, A.J. Anderson, L.B. Jakeman, D.M. McTigue, P.G. Popovich, Basso Mouse Scale for locomotion detects differences in recovery after spinal cord injury in five common mouse strains, J. Neurotrauma 23 (5) (2006) 635–659.
[33] J. Wu, Z. Feng, L. Chen, Y. Li, H. Bian, J. Geng, Z.H. Zheng, X. Fu, Z. Pei, Y. Qin, L. Yang, Y. Zhao, K. Wang, R. Chen, Q. He, G. Nan, X. Jiang, Z.N. Chen, P. Zhu, TNF antagonist sensitizes synovial fibroblasts to ferroptotic cell death in collagen-induced arthritis mouse models, Nat. Commun. 13 (1) (2022) 676.
[34] Z. Xiao, B. Kong, J. Fang, T. Qin, C. Dai, W. Shuai, H. Huang, Ferrostatin-1 alleviates lipopolysaccharide-induced cardiac dysfunction, Bioengineered 12 (2) (2021) 9367–9376.
[35] Y. Cao, Y. Li, C. He, F. Yan, J.R. Li, H.Z. Xu, J.F. Zhuang, H. Zhou, Y.C. Peng, X.J. Fu, X.Y. Lu, Y. Yao, Y.Y. Wei, Y. Tong, Y.F. Zhou, L. Wang, Selective ferroptosis inhibitor liproxstatin-1 attenuates neurological deficits and neuroinflammation after subarachnoid hemorrhage, Neurosci. Bull. 37 (4) (2021) 535–549.
[36] S. Hassanzadeh, M. Jalessi, S.B. Jameie, M. Khanmohammadi, Z. Bagher, Z. Namjoo, S.M. Davachi, More attention on glial cells to have better recovery after spinal cord injury, Biochem Biophys Rep 25 (2021) 100905.
[37] L.R. Watkins, E.D. Milligan, S.F. Maier, Glial proinflammatory cytokines mediate exaggerated pain states: implications for clinical pain, Adv. Exp. Med. Biol. 521 (2003) 1–21.
[38] T.M. Tsarouchas, D. Wehner, L. Cavone, T. Munir, M. Keatinge, M. Lambertus, A. Underhill, T. Barrett, E. Kassapis, N. Ogryzko, Y. Feng, T.J. van Ham, T. Becker, C.G. Becker, Dynamic control of proinflammatory cytokines Il-1beta and Tnf-alpha by macrophages in zebrafish spinal cord regeneration, Nat. Commun. 9 (1) (2018) 4670.
[39] C. Li, Z. Wu, L. Zhou, J. Shao, X. Hu, W. Xu, Y. Ren, X. Zhu, W. Ge, K. Zhang, J. Liu, R. Huang, J. Yu, D. Luo, X. Yang, W. Zhu, R. Zhu, C. Zheng, Y.E. Sun, L. Cheng, Temporal and spatial cellular and molecular pathological alterations with single-cell resolution in the adult spinal cord after injury, Signal Transduct. Targeted Ther. 7 (1) (2022) 65.
[40] S. Wahane, X. Zhou, X. Zhou, L. Guo, M.S. Friedl, M. Kluge, A. Ramakrishnan, L. Shen, C.C. Friedel, B. Zhang, R.H. Friedel, H. Zou, Diversified transcriptional responses of myeloid and glial cells in spinal cord injury shaped by HDAC3 activity, Sci. Adv. 7 (9) (2021).
[41] F.H. Brennan, Y. Li, C. Wang, A. Ma, Q. Guo, Y. Li, N. Pukos, W.A. Campbell, K.G. Witcher, Z. Guan, K.A. Kigerl, J.C.E. Hall, J.P. Godbout, A.J. Fischer, D. M. McTigue, Z. He, Q. Ma, P.G. Popovich, Microglia coordinate cellular interactions during spinal cord repair in mice, Nat. Commun. 13 (1) (2022) 4096.
[42] T. Zrzavy, C. Schwaiger, I. Wimmer, T. Berger, J. Bauer, O. Butovsky, J.M. Schwab, H. Lassmann, R. Hoftberger, Acute and non-resolving inflammation associate with oxidative injury after human spinal cord injury, Brain 144 (1) (2021) 144–161.
[43] D.J. Hellenbrand, C.M. Quinn, Z.J. Piper, C.N. Morehouse, J.A. Fixel, A.S. Hanna, Inflammation after spinal cord injury: a review of the critical timeline of signaling cues and cellular infiltration, J. Neuroinflammation 18 (1) (2021) 284.
[44] F. Liu, Y. Huang, H. Wang, Rodent models of spinal cord injury: from pathology to application, Neurochem. Res. 48 (2) (2023) 340–361.
[45] A. Kroner, A.D. Greenhalgh, J.G. Zarruk, R. Passos Dos Santos, M. Gaestel, S. David, TNF and increased intracellular iron alter macrophage polarization to a detrimental M1 phenotype in the injured spinal cord, Neuron 83 (5) (2014) 1098–1116.
[46] M. Wang, G. Tang, C. Zhou, H. Guo, Z. Hu, Q. Hu, G. Li, Revisiting the intersection of microglial activation and neuroinflammation in Alzheimer's disease from the perspective of ferroptosis, Chem. Biol. Interact. 375 (2023) 110387.